Available online at www.sciencedirect.com

SCIENCE DIRECT®

Polymer 45 (2004) 1313–1320

polymer

www.elsevier.com/locate/polymer

A RIS treatment of the mean-square dipole moment of PMMA chains in consideration of the pendant ester group orientations

Zhiping Zhou, Akihiro Abe*

Department of Applied Chemistry, Tokyo Institute of Polytechnics, 1583 Iiyama, Atsugi-shi 243-0297, Japan

Received 19 February 2003; received in revised form 25 March 2003; accepted 27 March 2003

Abstract

According to the six-state scheme proposed by Vacatello and Flory, the mean-square dipole moments $\langle M^2\rangle/x$ (x : number of monomeric units) of poly(methyl methacrylate) (PMMA) chains and their temperature dependence $\mathrm{d}\ln\langle M^2\rangle/\mathrm{d}T$ were calculated by the matrix algebra method of rotational isomeric state theory. To take account of the orientation effect of polar ester groups, the statistical weight matrices, U' and U'', were recast into an expanded form. A Bernoullian probability λ introduced to measure the preference between the two alternative orientations ($\chi = 0$ and $\chi = \pi$) of the side ester groups was found to give rise to a large effect on the mean-square dipole moment of polymers. When the skeletal bonds of a *meso* dyad are both in *trans*, an exceptionally strong dipole-dipole interaction may take place. If the two adjacent ester groups adopt the same orientation, the dipoles must be situated nearly parallel to each other in a close proximity. Such repulsive interactions may be alleviated by taking a staggered conformation, i.e. $(\chi, \chi') = (0, \pi)$ or $(\pi, 0)$. Such neighbor-dependent correlation inherent to the *meso* dyad is considered by assigning a parameter λ' to the proper element of the U_m'' matrix. The values of $\langle M^2\rangle/x$ observed at 30 °C were satisfactorily reproduced by adopting $\lambda = 0.270$ and $\lambda' = 0.865$. The thermal coefficients $\mathrm{d}\ln\langle M^2\rangle/\mathrm{d}T$ were found to be reconciled with the available experimental data by allowing the orientation parameters λ and λ' to be slightly temperature dependent. The stereochemical characteristics of the chain terminals were examined in order to extend the treatment to include the dipole moment of PMMA oligomers.

Keywords: Dipole moment; Rotational isomeric state model; Poly(methyl methacrylate)

1. Introduction

The mean-square dipole moment of polymer chains, $\langle M^2\rangle$, is a conformation-dependent property equivalent to the unperturbed chain dimension, the mean-square end-to-end distance, $\langle r^2\rangle$, and the mean-square radius of gyration, $\langle S^2\rangle$. The matrix algebra method [1–3] is available for the theoretical treatment of these quantities within the framework of the rotational isomeric state (RIS) approximation. The theoretical investigation of the poly(methyl methacrylate) (PMMA) chains was first reported by Sundararajan et al. [4]. On the basis of the conformational energy calculation, they proposed a two-state scheme by ignoring the high-energy *gauche* conformer designated as $\bar{g}$. This two-state model has been adopted by many authors to interpret experimental data of various conformation-dependent properties including SAXS [5], SANS [5], WAXS [6], and persistence vectors [7]. However O'Reilly et al. [8] reported that the results of their FTIR investigations on a blend sample comprising hydrogenous and deuterated PMMA could not be reconciled with the two-state scheme. Subsequently Sundararajan [9,10] proposed a revised (three-state) scheme in which the $\bar{g}$ state is allowed to occur. On the basis of some elaborate conformational energy calculations, Vacatello and Flory [11] proposed a six-state scheme to represent the internal rotation around the skeletal bonds, assigning the torsional energy minima at $-20°(t_-)$, $10°(t_+)$, $100°(g_-)$, $125°(g_+)$, $-125°(\bar{g}_-)$ and $-100°(\bar{g}_+)$. Due to severe steric conflicts, bond angles are substantially skewed: (1) the intradiad bond angles are assumed to be $\tau' = 124 \pm 1°$ for all conformers, and (2) the interdiad bond angles are taken to be $\tau = 106°$ when both adjoining skeletal bonds are *trans*, $\tau = 111°$ when one bond is t and the other g or $\bar{g}$, and $\tau = 116°$ when both are g or $\bar{g}$. The experimental results of the unperturbed dimension and

---

* Corresponding author. Tel./fax: +81-46-242-9536.
E-mail address: aabe@chem.t-kougei.ac.jp (A. Abe).

0032-3861/$ - see front matter © 2003 Elsevier Ltd. All rights reserved.
doi:10.1016/j.polymer.2003.03.001

their temperature coefficients were found to be well reproduced by the calculation according to the six-state scheme. In studying the molecular scattering functions, Vacatello et al. [12] concluded that the six-state RIS scheme provided the most satisfactory agreement with the available X-ray and neutron scattering results on both stereoregular and atactic PMMA samples over a wide range of scattering angle. In this work, we adopt the six-state scheme for the treatment of dielectric properties of PMMA.

A portion of the PMMA chain is depicted in Fig. 1. The ester group is conventionally assumed to be planar and $C^*{=}O^*$ is *cis* to the $O{-}CH_3$. The rotation of the ester group around the $C^\alpha{-}C^*$ bond is specified by angle χ: $\chi = 0$ to the *cis* conformation in which $C^*{=}O^*$ eclipses the $C^\alpha{-}CH_3$, and $\chi = \pi$ to the *trans* when these two bonds are *trans* to each other. Since the polar group is situated in the pendant side chains, the statistical mechanical averages must be taken over all conformations in consideration of the rotation (χ) around the first articulated bond. In the calculation of geometrical properties such as $\langle r^2 \rangle$ or $\langle S^2 \rangle$, the rotation of flexible side chains can be ignored.

For the sake of simplicity, an effective dipole moment assigned to each monomeric unit has been used as an approximation in estimating the mean-square moment of the polymeric system [13–15]. In such treatment, the details of the $C^\alpha{-}C^*$ rotation (χ) were ignored. A revised RIS scheme, which is applicable to the polymer chain having polar side groups, has been developed some time ago by one of the present authors [16–18]. The dipole moment of poly(vinyl ether)s has been rigorously treated in this manner [18,19]. In this work, we have derived a modified matrix algebra scheme, which allows us to estimate the mean-square dipole moment of the PMMA chains without resort to the pre-averaging method.

Experimental results of the dipole moment of PMMA chains are abundantly available in the literature [20–24]. Some of the former values are however somewhat obscure regarding the stereochemical composition of the sample. More recently Shima et al. [24] carried out dielectric measurements on two PMMA samples with well-defined tacticities: isotactic (iso-) PMMA ($2.13\ \mathrm{D}^2$) exhibited a higher mean-square dipole moment than syndiotactic (syn-) PMMA ($1.79\ \mathrm{D}^2$) in benzene at 30 °C. Ando et al. [23] studied dielectric properties of iso-, and atactic (at-) PMMA samples as a function of the degree of polymerization (DP). In the latter paper, the asymptotic behaviors of the mean-square dipole moment ratios are interpreted in terms of the helical wormlike chain theory.

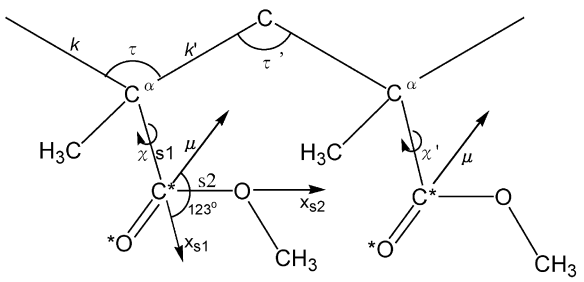

Fig. 1. Portion of a PMMA chain having a planar *trans* conformation.

2. Theoretical framework

We adopt essentially the same notations of the geometrical parameters as used in Ref. [11]. The location of the kth α-carbon C^α along the chain is defined by the serial index k. This index also identifies the kth interdiad junction. Accordingly, we specify the two skeletal bonds at the interdiad k by $k|k'$ and their internal rotations by $\varphi_k|\varphi_{k'}$. For consistency, χ_k is used to denote the torsional rotation around the kth side bond $C^\alpha{-}C^*$. The chiral character of given skeletal bonds and the associated reference frames is defined according to the traditional method [1–3], i.e. a d- or l-type bond is defined for the individual skeletal bond, and accordingly, the skeletal bonds k and k' shown in Fig. 1 may be identified as l- and d-type bond. Let $T(\theta, \varphi)$ and $T^*(\theta, \varphi)$ be the transformation matrices [1–3] for the adjacent frames of the same sense (either ll or dd) and those of the opposite sense (either ld or dl), respectively. Here θ is the supplement of the bond angle and φ the torsion angle of the bond under consideration. The reference frames attached to side bonds $C^\alpha{-}C^*$ and $C^*{-}O$, which were denoted as s_1 and s_2, respectively, are defined as follows. The axes x_{s_1} and x_{s_2} are taken to be in the directions of s_1 and s_2, respectively, and the y_{s_1}, y_{s_2} are chosen in the plane defined by skeletal bond k and side bond s_1, and by bonds s_1 and s_2, respectively. The same rule can be applied to define the chirality of the coordinate system for bonds s_1 and s_2. The transformation matrices required for treating the side chain orientation may be formulated as follows:

Transformation from frame s_2 to s_1

$$T_s = T(180° - \angle C^\alpha C^* O, \varphi_{s1} - \Delta\varphi_1) \tag{1}$$

and that from frame s_1 to skeletal bond k

$$T_0 = T(180° - \angle C C^\alpha C^*, \varphi_k - \Delta\varphi_2) \tag{2}$$

where $\Delta\varphi_1$ is the angle between the plane defined by the skeletal $CH_2{-}C^\alpha$ and the side $C^\alpha{-}C^*$ bond and the one defined by the $C^\alpha{-}C^*$ and the articulated $C^\alpha{-}CH_3$ bond, and $\Delta\varphi_2$ the angle between the plane defined by the skeletal $CH_2{-}C^\alpha$ and the $C^\alpha{-}CH_2$ bond and the one defined by the skeletal $CH_2{-}C^\alpha$ and the side $C^\alpha{-}C^*$ bond. In principle, these expressions are valid regardless of the chirality of bond k. When the pendant ester group takes the *cis* conformation, φ_{s1} equals 0. The displacement angles $\Delta\varphi_1$

and $\Delta\varphi_2$ are given by

$$\cos\Delta\varphi_1 = \frac{\cos\angle \mathrm{CC^{\alpha}(CH_3)} - \cos\angle \mathrm{CC^{\alpha}C^{*}}\cos\angle \mathrm{(CH_3)C^{\alpha}C^{*}}}{\sin\angle \mathrm{CC^{\alpha}C^{*}}\sin\angle \mathrm{(CH_3)C^{\alpha}C^{*}}} \tag{3}$$

$$\cos\Delta\varphi_2 = \frac{\cos\angle \mathrm{CC^{\alpha}C^{*}}(1-\cos\angle \mathrm{CC^{\alpha}C})}{\sin\angle \mathrm{CC^{\alpha}C^{*}}\sin\angle \mathrm{CC^{\alpha}C}} \tag{4}$$

A value of 120° was used for $\Delta\varphi_1$ in this work.

According to Saiz et al. [25], the dipole moment of the ester group, μG, is located in the ester plane and directed at an angle about 123° from x_{s_1}, which is nearly antiparallel to the $\mathrm{C^{*}{=}O^{*}}$ bond (cf. Fig. 1). In the Cartesian coordinate system affixed to s_2, the dipole moment of the ester group may be expressed as

$$\boldsymbol{\mu} = \begin{pmatrix} \mu_0\cos 57^{\circ} \\ -\mu_0\sin 57^{\circ} \\ 0 \end{pmatrix} \tag{5}$$

where $\mu_0 = 1.73$ D corresponds to the magnitude of the dipole moment of the ester group [22]. The contribution from the aliphatic C–C bonds to the dielectric properties is assumed to be nil. The dipole moment of the ester group can be expressed in the coordinate system defined for skeletal bond k as

$$\mathbf{m} = T_0 T_{\mathrm{s}}\boldsymbol{\mu} \tag{6}$$

According to the formulation given by Flory et al. [1–3], the mean-square dipole moment for a polymer chain is given by

$$\langle M^2\rangle = Z^{-1} g_0\left(\prod_{k=1}^{x-1} g'_k g''_k\right) g_x \tag{7}$$

where gs are called the generator matrix, and g_0 and g_x are respective row and column matrices for the two terminal bonds, and Z is the conformational partition function. The g matrix was originally formulated for polymer chains carrying dipoles tightly fixed onto the skeletal bond by the G-matrix

$$G_k = \begin{pmatrix} 1 & 2\mathbf{m}^{\mathrm{T}}T & m^2 \\ 0 & T & \mathbf{m} \\ 0 & 0 & 1 \end{pmatrix}_k \tag{8}$$

For the first bond of every dyad, $m \equiv 0$. The generator matrix may be expressed as

$$g_k = ((U \otimes E_5)\|G\|)_k \tag{9}$$

where E_5 is the identity matrix of order five, U the statistical weight matrix, and $\|G\|_k$ may be derived by prescribing G matrices for the appropriate rotational states of bond k assembled in the diagonal array.

The expression given in Eq. (7) can be easily expanded to accommodate the rotational characteristics of the side groups as required in the treatment of the dipole moment of PMMA, and the alternative orientation of the ester group between the two states ($\chi = 0$ or π) can be taken into account by the following expression

$$\langle M^2\rangle = Z^{-1}(\lambda g_0(0)\ (1-\lambda)g_0(\pi)) \times \left(\prod_{k=1}^{x-1}\begin{pmatrix} g'_k & \\ & g'_k \end{pmatrix}\begin{pmatrix} \lambda g''_k(0) & (1-\lambda)g''_k(\pi) \\ \lambda g''_k(0) & (1-\lambda)g''_k(\pi) \end{pmatrix}\right) \times \begin{pmatrix} g_x \\ g_x \end{pmatrix} \tag{10}$$

where $g(0)$ and $g(\pi)$ represent, respectively, the generator matrices defined for the orientation $\chi = 0$ and π. Bernoullian probabilities are introduced to consider the preference between these orientations: λ for $\chi = 0$ and accordingly $(1-\lambda)$ for $\chi = \pi$.

As easily shown by a proper model, an exceptionally strong dipole–dipole interaction may takes place when the two successive skeletal bonds of a *meso* dyad are in the *trans–trans* state (Fig. 1). If the two adjacent ester groups take the same orientation, i.e. $(\chi, \chi') = (0,0)$ or (π,π), the dipoles must be situated nearly parallel to each other at a separation of only ca. 2.5 Å. An alternate orientation such as $(\chi,\chi') = (0,\pi)$ or $(\pi, 0)$ would be more favorable in the *tt* state. Following the previous notation, we assign a probability λ' to the alternate orientation and, accordingly, $1-\lambda'$ to the synchronized arrangement for the *tt* state of *meso* dyad. These considerations may be taken into account by expanding the statistical weight matrices (see Eq. (11) overleaf) where $u_{t\_t_-}$, $u_{t\_t_+}$, etc are the respective elements of U''_m. Accordingly, the associated matrix U' should be also expanded to a 12×12 form comprising a quasi-diagonal array of the original matrix.

$$\tilde{U}' = \begin{pmatrix} U' & \\ & U' \end{pmatrix} \tag{12}$$

3. Oligomers and the end effect

Ando et al. [23,26] have reported the dipole moment data for oligomeric PMMA samples. The oligomers prepared by the group-transfer polymerization possess hydrogen atoms at both ends, leading to the chemical constitution such as shown in Fig. 2. Following the definition of the bond order given in Fig. 1, serial numbers are used in specifying the order of the constituent skeletal bonds: i.e. $1, 1', 2, 2' \ldots, x$ and x'. To facilitate the treatment, we take the first $\mathrm{C^{*}{-}C^{\alpha}}$ bond (labeled 1) as the initial bond of the chain sequence, and accordingly the last $\mathrm{C^{\alpha}{-}C^{*}}$ bond (x') to terminate the chain.

Conformational energy calculations and the subsequent dipole moment analysis of dimethyl esters of dicarboxylic acids, $\mathrm{CH_3OC^{*}(O^{*})(CH_2)_{\mathit{n}}C^{*}(O^{*})OCH_3}$ ($n = 1$–4 or 8),

$$\tilde{\mathrm{U}}''_{\mathrm{m}} = \begin{array}{c|c} & \begin{array}{cccc} \multicolumn{2}{c}{\overline{\qquad\qquad\qquad 0 \qquad\qquad\qquad}} & \multicolumn{2}{c}{\overline{\qquad\qquad\qquad \pi \qquad\qquad\qquad}} \end{array} \\ \begin{array}{c} 0 \\ \\ \pi \\ \\ \end{array} & \left(\begin{array}{cccc} (1-\lambda')\lambda \begin{pmatrix} u_{t_-t_-} & u_{t_-t_+} \\ u_{t_+t_-} & u_{t_+t_+} \end{pmatrix} & 0.5\lambda \begin{pmatrix} u_{t_-g_-} & u_{t_-g_+} & u_{t_-\bar{g}_-} & u_{t_-\bar{g}_+} \\ u_{t_+g_-} & u_{t_+g_+} & u_{t_+\bar{g}_-} & u_{t_+\bar{g}_+} \end{pmatrix} & \lambda'(1-\lambda) \begin{pmatrix} u_{t_-t_-} & u_{t_-t_+} \\ u_{t_+t_-} & u_{t_+t_+} \end{pmatrix} & 0.5(1-\lambda) \begin{pmatrix} u_{t_-g_-} & u_{t_-g_+} & u_{t_-\bar{g}_-} & u_{t_-\bar{g}_+} \\ u_{t_+g_-} & u_{t_+g_+} & u_{t_+\bar{g}_-} & u_{t_+\bar{g}_+} \end{pmatrix} \\ 0.5\lambda \begin{pmatrix} u_{g_-t_-} & u_{g_-t_+} \\ u_{g_+t_-} & u_{g_+t_+} \\ u_{\bar{g}_-t_-} & u_{\bar{g}_-t_+} \\ u_{\bar{g}_+t_-} & u_{\bar{g}_+t_+} \end{pmatrix} & 0.5\lambda \begin{pmatrix} u_{g_-g_-} & u_{g_-g_+} & u_{g_-\bar{g}_-} & u_{g_-\bar{g}_+} \\ u_{g_+g_-} & u_{g_+g_+} & u_{g_+\bar{g}_-} & u_{g_+\bar{g}_+} \\ u_{\bar{g}_-g_-} & u_{\bar{g}_-g_+} & u_{\bar{g}_-\bar{g}_-} & u_{\bar{g}_-\bar{g}_+} \\ u_{\bar{g}_+g_-} & u_{\bar{g}_+g_+} & u_{\bar{g}_+\bar{g}_-} & u_{\bar{g}_+\bar{g}_+} \end{pmatrix} & 0.5(1-\lambda) \begin{pmatrix} u_{g_-t_-} & u_{g_-t_+} \\ u_{g_+t_-} & u_{g_+t_+} \\ u_{\bar{g}_-t_-} & u_{\bar{g}_-t_+} \\ u_{\bar{g}_+t_-} & u_{\bar{g}_+t_+} \end{pmatrix} & 0.5(1-\lambda) \begin{pmatrix} u_{g_-g_-} & u_{g_-g_+} & u_{g_-\bar{g}_-} & u_{g_-\bar{g}_+} \\ u_{g_+g_-} & u_{g_+g_+} & u_{g_+\bar{g}_-} & u_{g_+\bar{g}_+} \\ u_{\bar{g}_-g_-} & u_{\bar{g}_-g_+} & u_{\bar{g}_-\bar{g}_-} & u_{\bar{g}_-\bar{g}_+} \\ u_{\bar{g}_+g_-} & u_{\bar{g}_+g_+} & u_{\bar{g}_+\bar{g}_-} & u_{\bar{g}_+\bar{g}_+} \end{pmatrix} \\ \lambda'\lambda \begin{pmatrix} u_{t_-t_-} & u_{t_-t_+} \\ u_{t_+t_-} & u_{t_+t_+} \end{pmatrix} & 0.5\lambda \begin{pmatrix} u_{t_-g_-} & u_{t_-g_+} & u_{t_-\bar{g}_-} & u_{t_-\bar{g}_+} \\ u_{t_+g_-} & u_{t_+g_+} & u_{t_+\bar{g}_-} & u_{t_+\bar{g}_+} \end{pmatrix} & (1-\lambda')(1-\lambda) \begin{pmatrix} u_{t_-t_-} & u_{t_-t_+} \\ u_{t_+t_-} & u_{t_+t_+} \end{pmatrix} & 0.5(1-\lambda) \begin{pmatrix} u_{t_-g_-} & u_{t_-g_+} & u_{t_-\bar{g}_-} & u_{t_-\bar{g}_+} \\ u_{t_+g_-} & u_{t_+g_+} & u_{t_+\bar{g}_-} & u_{t_+\bar{g}_+} \end{pmatrix} \\ 0.5\lambda \begin{pmatrix} u_{g_-t_-} & u_{g_-t_+} \\ u_{g_+t_-} & u_{g_+t_+} \\ u_{\bar{g}_-t_-} & u_{\bar{g}_-t_+} \\ u_{\bar{g}_+t_-} & u_{\bar{g}_+t_+} \end{pmatrix} & 0.5\lambda \begin{pmatrix} u_{g_-g_-} & u_{g_-g_+} & u_{g_-\bar{g}_-} & u_{g_-\bar{g}_+} \\ u_{g_+g_-} & u_{g_+g_+} & u_{g_+\bar{g}_-} & u_{g_+\bar{g}_+} \\ u_{\bar{g}_-g_-} & u_{\bar{g}_-g_+} & u_{\bar{g}_-\bar{g}_-} & u_{\bar{g}_-\bar{g}_+} \\ u_{\bar{g}_+g_-} & u_{\bar{g}_+g_+} & u_{\bar{g}_+\bar{g}_-} & u_{\bar{g}_+\bar{g}_+} \end{pmatrix} & 0.5(1-\lambda) \begin{pmatrix} u_{g_-t_-} & u_{g_-t_+} \\ u_{g_+t_-} & u_{g_+t_+} \\ u_{\bar{g}_-t_-} & u_{\bar{g}_-t_+} \\ u_{\bar{g}_+t_-} & u_{\bar{g}_+t_+} \end{pmatrix} & 0.5(1-\lambda) \begin{pmatrix} u_{g_-g_-} & u_{g_-g_+} & u_{g_-\bar{g}_-} & u_{g_-\bar{g}_+} \\ u_{g_+g_-} & u_{g_+g_+} & u_{g_+\bar{g}_-} & u_{g_+\bar{g}_+} \\ u_{\bar{g}_-g_-} & u_{\bar{g}_-g_+} & u_{\bar{g}_-\bar{g}_-} & u_{\bar{g}_-\bar{g}_+} \\ u_{\bar{g}_+g_-} & u_{\bar{g}_+g_+} & u_{\bar{g}_+\bar{g}_-} & u_{\bar{g}_+\bar{g}_+} \end{pmatrix} \end{array} \right) \end{array} \tag{11}$$

have been reported by one of the present authors [27]. For these compounds, the internal rotation around the skeletal $C^*{-}C$ bond is most controversial. When the ester groups are allowed to take conformations in which either the carbonyl $C^*{=}O^*$ or the ether $C^*{-}O$ bond eclipses the aliphatic C–C bond or C–H bonds joining the same α-carbon, the statistical weight matrix inevitably becomes a six-state scheme. In the PMMA oligomers under consideration, every C^{α} carbon carries two methyl groups. Since the CH_3 and CH_2 groups are nearly equivalent in size, the statistical weight matrix of the first bond may be formulated in a 1 × 6 array in the order $2\pi/3$, $-2\pi/3$, 0, $\pi/3$, $-\pi/3$, π :

$$U_1 = \begin{pmatrix} \alpha & \alpha & \alpha & 1-\alpha & 1-\alpha & 1-\alpha \end{pmatrix} \tag{13}$$

Here a Bernoullian probability α is assigned to the conformation (*cis*) in which $C^*{=}O^*$ is eclipsing C–C bond.

For the statistical weight of the rotation around bond 1′, Eq. (4) of Ref. [27] may be applicable provided that the steric interactions involving the two CH_3 groups situated on the C^{α} carbon are taken into account. A value of $\sigma = \exp(-E_{\sigma}/RT)$ with $E_{\sigma} = 2.1\ \mathrm{kJ\ mol^{-1}}$ has been adopted tentatively in consideration of the *gauche* interaction encountered in the *n*-alkane chain [28]. In Ref. [27], the *tt* conformation was taken to be the reference for the consecutive $C^*{-}C_1{-}C_2$ bond rotations at the terminal of the dicarboxylic acid ester: i.e. the carbonyl $C^*{=}O^*$ group eclipses the $C_1{-}C_2$ bond. Since the carbonyl groups are situated in the side chain in the PMMA chain, the reference states must be redefined when the two molecular systems are compared. As shown by a proper molecular model, the geometrical equivalence of the torsion angles 0, $2\pi/3$ and $-2\pi/3$ of the $C^*{-}C_1$ bond in Ref. [27] are, respectively, found at $-2\pi/3$, $2\pi/3$, and 0 around bond 1 ($C^*{-}C^{\alpha}$) in this work. Similarly, the rotational minima at 0, $2\pi/3$, and $-2\pi/3$ of the $C_1{-}C_2$ bond in Ref. [27] should, respectively, correspond to those at $2\pi/3$, $-2\pi/3$, and 0 of bond 1′ in the present scheme. All these considerations are put together in the prescription of the $U_{1'}$ matrix

$$U_{1'} = \begin{pmatrix} 0 & \sigma & \xi_1 \\ \xi_3 & \sigma & \xi_3 \\ \xi_1 & \sigma & 0 \\ \xi_3 & \sigma & \xi_3 \\ 0 & \sigma & \xi_1 \\ \xi_1 & \sigma & 0 \end{pmatrix} \tag{14}$$

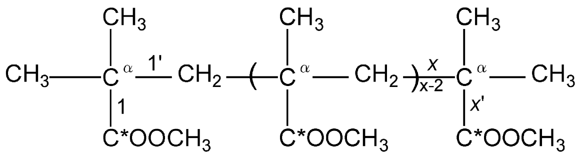

$CH_3{-}C^{\alpha}(CH_3)(C^*OOCH_3){-}CH_2{-}(C^{\alpha}(CH_3)(C^*OOCH_3){-}CH_2)_{x-2}{-}C^{\alpha}(CH_3)(C^*OOCH_3){-}CH_3$

Fig. 2. A schematic diagram of the PMMA chain. The first side $C^*{-}C^{\alpha}$ bond is numbered as 1 and the last side $C^{\alpha}{-}C^*$ bond as x'.

The alternative orientations (*cis* and *trans*) of the ester group are taken into account by adopting six states for bond 1 (rows), where the relative weight of the *cis* conformation has been considered by a factor α in Eq. 13. In Eq. 14, columns are indexed in the order t, g, and $\bar{g}$ around bond 1′, and $\xi_i = \exp(-E_{\xi_i}/RT)$ with $E_{\xi 1} = -0.59\ \mathrm{kJ\ mol^{-1}}$ and $E_{\xi 3} = 1.63\ \mathrm{kJ\ mol^{-1}}$, which represent the interaction similar to those defined in Ref. [27].

Following Vacatello and Flory [11], we may adopt the expanded six-state scheme for bond 1′: i.e. −20°(t_-), 10°(t_+), 100°(g_-), 125°(g_+), −125°($\bar{g}_-$) and −100°($\bar{g}_+$). The $U_{1'}$ matrix (Eq. (14)) must be accordingly expanded to a 6 × 6 scheme by this revision. The $U_{x'}$ matrix for the other terminal should take a form such as

$$U_{x'} = \begin{pmatrix} \alpha & \alpha & \alpha & 1-\alpha & 1-\alpha & 1-\alpha \\ \alpha & \alpha & \alpha & 1-\alpha & 1-\alpha & 1-\alpha \\ \alpha & \alpha & \alpha & 1-\alpha & 1-\alpha & 1-\alpha \\ \alpha & \alpha & \alpha & 1-\alpha & 1-\alpha & 1-\alpha \\ \alpha & \alpha & \alpha & 1-\alpha & 1-\alpha & 1-\alpha \\ \alpha & \alpha & \alpha & 1-\alpha & 1-\alpha & 1-\alpha \end{pmatrix} \qquad (15)$$

where the columns are arranged in the order $2\pi/3$, $-2\pi/3$, 0, $\pi/3$, $-\pi/3$, π for the last C^{α}–C^{*} bond (x'). A special consideration may be required for the terminal *meso* dyad: i.e. when bonds $1'$ and 2 simultaneously adopt the *trans* conformation, the $\pm 2\pi/3$ and $\pm\pi/3$ states of the ester group around bond 1 must be suppressed by the severe steric interaction with the adjacent ester groups, leaving two alternative states, 0, and π, for the bond. A similar consideration applies to the opposite end. Some trial calculations indicate that the value of α has little effect on the mean-square dipole moment. Thus otherwise noted, we choose $\alpha = 0.5$ in this work.

Vacatello and Flory [11] estimated a priori probabilities of the *trans* state for the inner bonds involved in the isotactic and syndiotactic chains, respectively: $f_i = 0.718$ and $f_s = 0.886$ at 300 K. In both cases, the fraction of the *trans* state is much higher than those of the *gauche* arrangements. As shown by the manipulation of a model, the bond rotation around the terminal bonds labeled 2 and x may be somewhat less restricted than those of the corresponding inner bonds, leading to an enhancement of the *gauche* probability. In order to take this effect into account, the statistical weights associated with the *gauche* states of bonds 2 and x are multiplied by a factor η. The factor should have no significance for the long polymeric chains.

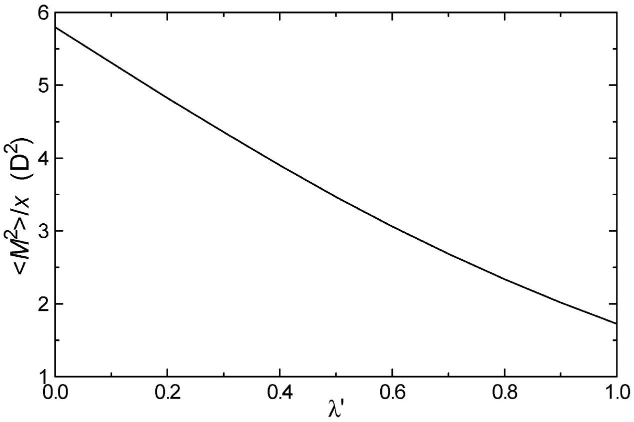

Fig. 4. The dependence of the mean-square dipole moment $\langle M^2\rangle/x$ on the orientation correlation probability, λ', assigned to the *tt* state of the *meso* dyad. Calculations were carried out for the perfectly isotactic PMMA chains of 1000 units at 30 °C, the orientation probability, λ, being set equal to 0.270.

4. Results

We have first calculated the mean-square dipole moment as a function of the probability λ for the stereoregular PMMA chains with the degree of polymerization $x = 1000$. Our trial calculations indicate that the interdiad bond angle τ has little effect on the mean-square dipole moment $\langle M^2\rangle/x$. The averaged value of 108° was adopted for angle τ throughout the present work. The results obtained for the temperature of 30 °C are shown in Fig. 3. The dipole moment appreciably depends on the orientation of the articulated side bonds for both iso- and syn-PMMA chains. The agreement with experimental results [23,24] is found to be reasonable for syn-PMMA at around $\lambda = 0.270$. For the iso-PMMA chain, however, the calculated dipole moment substantially exceeds experimental values over the whole range

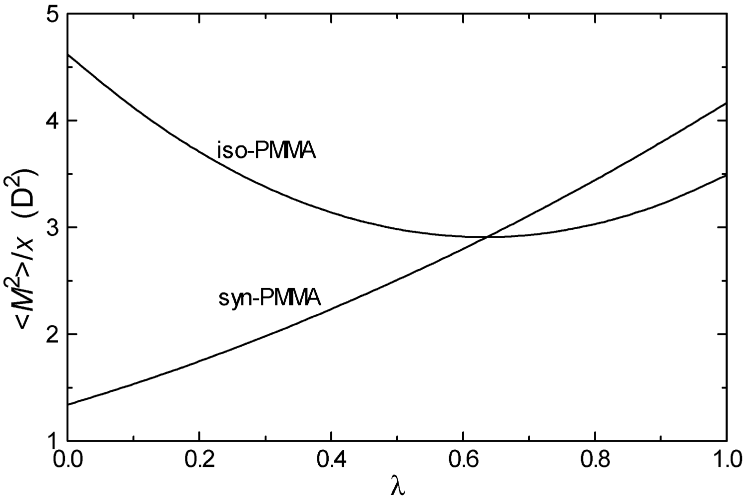

Fig. 3. The dependence of the mean-square dipole moment $\langle M^2\rangle/x$ on the orientation probability of ester groups, λ, calculated for the perfectly isotactic and syndiotactic PMMA chains comprising 1000 units at 30 °C. The orientation correlation parameter, λ' for the *meso* dyad was kept constant (0.5).

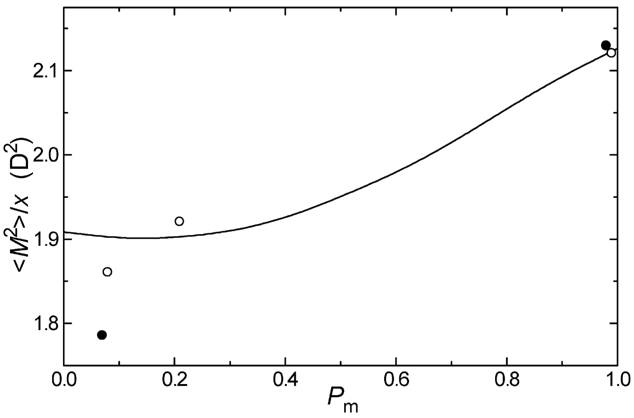

Fig. 5. Variation of the mean-square dipole moment $\langle M^2\rangle/x$ as a function of the *meso*-dyad content (P_m). The solid curve represents the results of calculation for Monte Carlo chains of 1000 units, with $\lambda = 0.270$ and $\lambda' = 0.865$. The experimental data (in benzene 30 °C) reported by Ando et al. [23] and Shima et al. [24] are, respectively, shown by open and filled circles.

of λ. The effect of λ' was then examined for the iso-PMMA chain, λ being kept at 0.270. As shown in Fig. 4, the mean-square dipole moment $\langle M^2\rangle/x$ varies from 5.79 to 1.72 D^2 with an increase of $\lambda' = 0$ to 1. The observed value ($\sim$2.13 D^2) [23,24] is reproduced around $\lambda' = 0.865$.

In Fig. 5, the mean-square dipole moment of atactic PMMA chains is plotted against the stereochemical constitution expressed by the fraction of *meso* dyad, P_m, at 30 °C. Calculations were carried out for stereochemical sequences of 1000 units generated by the Monte Carlo technique [1]. The distribution of the *meso* and *racemic* dyads along the chain is Bernoullian. The averages were taken over 100 Monte Carlo chains for given values of P_m. In all these calculations, the probabilities representing the orientation of the ester groups are taken to be identical: $\lambda = 0.270$ and $\lambda' = 0.865$. The theoretical curve thus derived is concave, showing a shallow minimum at about $P_m = 0.15$, in contrast to that reported for the mean-square end-to-end distance [11]. Some recent experimental data [23,24] obtained for PMMA samples with well-defined tacticity are also included in the figure. Although the experimental data are scattered, the agreement is reasonable.

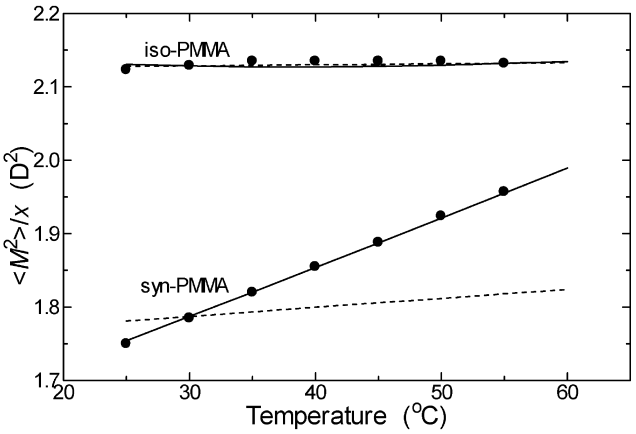

Fig. 6. The temperature dependence of the mean-square dipole moment $\langle M^2\rangle/x$. The broken curves represent the results calculated by using fixed values of $\lambda = 0.214$ and $\lambda' = 0.883$ at all temperatures. The solid curves are those obtained by assuming the orientation parameters to vary with temperature: $\lambda = 0.214 + 0.272 \times 10^{-2}(T - 30)$ and $\lambda' = 0.883 – 0.920 \times 10^{-3}(T - 30)$, T being the temperature in °C. Experimental data of Shima et al. [24] are indicated by filled circles (measured in benzene).

To facilitate comparison with the experimental results reported by Shima et al. [24], the temperature dependence of the $\langle M^2\rangle/x$ value was examined for the PMMA sequence with $P_m = 0.98$ and 0.07, respectively, for the isotactic and syndiotactic chain (Fig. 6). To optimize the agreement between the calculated and experimental results, the values of λ and λ' are slightly adjusted. Shima et al.'s experimental results were most satisfactorily reproduced by adopting a set of values $\lambda = 0.214$ and $\lambda' = 0.883$ at the temperature of 30 °C. The dashed curves were derived by the calculation using these values of λ and λ' for the entire range of temperature: $\mathrm{d}\ln\langle M^2\rangle/\mathrm{d}T = 0.659 \times 10^{-4}\ \mathrm{K}^{-1}$ for iso-PMMA and $6.825 \times 10^{-4}\ \mathrm{K}^{-1}$ for syn-PMMA. As shown in Fig. 6, the slope of the calculated curve is much smaller than that observed for the syndiotactic chain. The discrepancy can be fixed by allowing the temperature dependence of the orientation probabilities λ and λ'. With increasing temperature, the rotation of the side bond should tend to be more activated, and, as the results, the magnitudes of λ and λ' should shift toward the equal probability of 0.5. The solid curves were derived by assuming λ and λ' to vary linearly from 0.214 to 0.282 and from 0.883 to 0.860, respectively, with the increase of temperature from 30 to 55 °C. The observed results were then satisfactorily reproduced for both iso-PMMA and syn-PMMA: $\mathrm{d}\ln\langle M^2\rangle/\mathrm{d}T = 0.608 \times 10^{-4}\ \mathrm{K}^{-1}$ for iso-PMMA and $3.592 \times 10^{-3}\mathrm{K}^{-1}$ for syn-PMMA.

Shown in Fig. 7 are the plots of the ratio $\langle M^2\rangle/x$ against $\log_{10} x$, the logarithm of DP. The solid and broken curves,

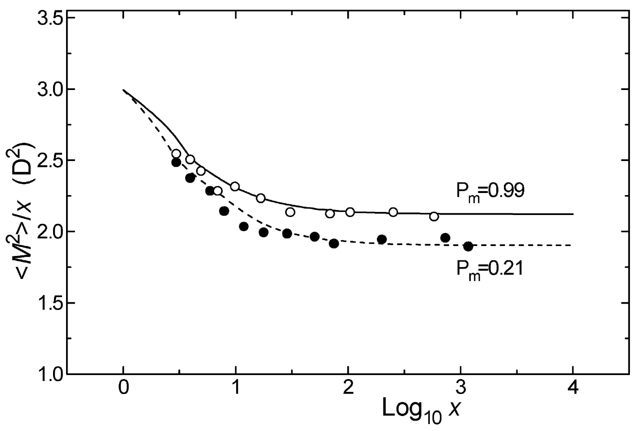

Fig. 7. Variation of $\langle M^2\rangle/x$ with DP ($\log_{10} x$). The solid curve represents the calculation for iso-PMMA with $P_m = 0.99$, and the broken curve for at-PMMA with $P_m = 0.21$. Experimental data of Ando et al. [23] are shown by open and filled circles, respectively, for iso- and at-PMMA.

respectively, indicate the results of calculation for chains having a highly isotactic ($P_m = 0.99$) and an atactic sequence ($P_m = 0.21$) for the temperature of 30 °C. The open and solid circles represent the experimental data reported by Ando et al. [23] for PMMA samples having tacticities, respectively, given above. In the calculation stated above, we have adopted a value of $\eta = 4$ to correct for the effect inherent to the terminal of the chain. Neglecting such terminal effects (i.e. $\eta = 1$), a dramatic peak appears at $x = 3$ for both iso- and syn-PMMA chains. With this modification ($\eta = 4$), the theoretical curves exhibit a good agreement with the experimental $\langle M^2 \rangle / x$ vs. $\log_{10} x$ plots, which tend to decrease monotonically with x, and then approach to the respective asymptotic limit: $(\langle M^2 \rangle / x)_{x \to \infty} = 2.13\ \mathrm{D}^2$ (iso-PMMA) and $1.91\ \mathrm{D}^2$ (syn-PMMA).

5. Discussion

Theoretical evaluation of the mean-square dipole moment of PMMA chains is not so abundant as the experimental measurement. The rotation-averaged dipole moment within the monomer unit and the two-state RIS scheme were used in the calculation by Birshtein et al. [13]. The experimental dependence of $\langle M^2 \rangle / x$ on x were well explained by Ando et al. [23] using the helical wormlike chain model. In their analysis, however, the orientation of the individual ester groups is entirely neglected. In this work, we have attempted to calculate the mean-square dipole moment by formulating an expanded RIS scheme which takes into account the orientation effect of the ester group in conjunction with the skeletal conformation of the PMMA chain. A Bernoullian probability λ was introduced to represent the orientation of the ester group either at the 0 or π position. Special attention was required for the *trans–trans* conformation of the *meso* dyad, where an alternate orientation of the two neighboring ester groups may be preferred. In order to take such neighbor-dependent character into account, the probability λ' has been appended to the appropriate elements of the $\tilde{U}''_m$. In order to reconcile the calculation with the experimental observations, a set of parameters such as $\lambda = 0.270$ and $\lambda' = 0.865$ were found to be adequate. A value of $\lambda = 0.270$ implies that the *trans* conformation is the preferred form of the ester group relative to *cis*: the energy difference amounts to 2.50 kJ mol^{-1} at 30 °C in terms of a simple Boltzmann expression. This result is in a qualitative agreement with the conclusion of Birshtein et al. [13]. Various spectroscopic studies have been carried out to elucidate the location of the most preferred conformation around the aliphatic ester bond –CC–C(O)O–. The experimental results are somewhat divergent however. In PMMA, the bulky pendant groups are sterically interacting with each other in most of the skeletal arrangements. The difference between the van der Waals volumes of the two oxygens may play a role in determining the stability of the ester conformation. The carbonyl oxygen is more anisotropic and has a larger van der Waals volume than the ether oxygen [29]. An inspection of a model should lead to a preferred arrangement in which the ether C–O bond eclipses the C–C bond (*cis*), thus $\lambda < 0.5$ in accord with our results. A value of $\lambda' = 0.865$ corresponds to an energy difference of 4.68 kJ mol^{-1} in terms of the Boltzmann expression, indicating that the two adjacent ester groups involved in the *meso* dyad prefer to take an alternate orientation with each other when the related skeletal bonds are both in *trans*. Such a cooperative effect inherent to the isotactic arrangement has been mentioned in Birshtein et al.'s work [13]. The energy difference estimated in our work is somewhat higher than that (1.67 kJ mol^{-1}) reported by Tarazona and Saiz [14] for poly(methyl acrylate) on the basis of the conventional RIS calculation.

According to the experimental results reported by Shima et al. [24], the temperature dependence of the dipole moment is quite divergent between the isotactic and syndiotactic chains. While the observed values of $\langle M^2 \rangle / x$ remain relatively insensitive to the temperature for iso-PMMA, a significant increase with temperature is observed for syn-PMMA. When fixed values are used for the orientation parameters λ and λ' throughout the temperature range examined, our RIS calculation gave somewhat lower estimate of $\mathrm{d}\ln\langle M^2 \rangle / \mathrm{d}T$ for syn-PMMA although the sign of the slope is correctly predicted. This discrepancy was found to be remedied by adjusting the parameters λ and λ'. A linear relation with temperature was assumed for both λ and λ' in the aforementioned calculation (see Fig. 6). If we tentatively adopt a Boltzmann expression such as $\zeta = A \times \exp(-E_\zeta / RT)$ with ζ representing $\lambda/(1 - \lambda)$ or $\lambda'/(1 - \lambda')$, the corrections required to improve the agreement with experimental observations amount to expressions $\lambda/(1 - \lambda) = 33.4 \exp(-12.1/RT)$ and $\lambda'/(1 - \lambda') = 0.51 \times \exp(6.8/RT)$, the energies being given in kJ mol^{-1}. The deviation of the pre-exponential factor from unity is substantial in both formulae. At this moment, however, we have no reasonable explanation to these numerical results.

In treating the dipole moment of PMMA oligomers, the terminal effect must be taken into account. As shown in Fig. 2, the ester groups situated at the end of the chain are less restricted and thus the available states for the end group should be more proliferated. The ester groups can easily choose either the *cis* or *trans* position around the –CC–C(O)O– bond at the terminals. In a tentative calculation, the parameter α representing this effect was varied from 0 to 1. For the simple aliphatic dicarboxylic acids, the energy difference between these two states was found to cause the even–odd character of the dipole moment with respect to the chain length [27]. In the present example, however, the dipole moment $\langle M^2 \rangle / x$ of the lower oligomers was found to remain nearly unaffected by the value of α: e.g. the increment of the dipole moment over the range $\alpha = 0$ to 1 is less than 2% at $x = 3$. The parameter η has been introduced somewhat arbitrarily to avoid an anomalous peak appearing at $x = 3$. The physical meaning of the parameter is not clear at this moment. In general, the rotational characteristics of the PMMA chain at the terminals are not well understood. Although a satisfactory reproduction of the experimental observations has been achieved in this paper, the statistical weight parameters adopted here must be refined in the forthcoming work.

Acknowledgements

This work was partially supported by the Grant-in-Aid for Scientific Research (13650959) through Monbukagakusho in Japan. One of the authors (ZZ) would like to express his gratitude for the Postdoctoral Fellowship for Foreign Researchers sponsored by the Japan Society for the Promotion of Science (JSPS), and he also thanks for the support by a Grant-in-Aid for Science Research (P01094) of Monbukagakusho. AA thanks Professors M. Shima and T. Yoshizaki for making their experimental data available to us at an early stage of the work.

References

[1] Flory PJ. Statistical mechanics of chain molecules. New York: Interscience; 1969.
[2] Flory PJ. Macromolecules 1974;7:381.
[3] Flory PJ, Sundararajan PR, DeBolt LC. J Am Chem Soc 1974;96:5015.
[4] Sundararajan PR, Flory PJ. J Am Chem Soc 1974;96:5025.
[5] Yoon DY, Flory PJ. Polymer 1975;16:645.
[6] Lovell R, Windle AH. Polymer 1981;22:175.
[7] Yoon DY, Flory PJ. J Polym Sci, Polym Phys Ed 1976;14:1425.
[8] O'Reilly JM, Mosher RA. Macromolecules 1981;14:602.
[9] Sundararajan PR. Macromolecules 1986;19:415.
[10] Sundararajan PR. Macromolecules 1979;12:575.
[11] Vacatello M, Flory PJ. Macromolecules 1986;19:405.
[12] Vacatello M, Yoon DY, Flory PJ. Macromolecules 1990;23:1993.
[13] Birshtein TM, Merkur'yeva AA, Goryunov AN. Polym Sci USSR 1983;25:143.
[14] Tarazona MP, Saiz E. Macromolecules 1983;16:1128.
[15] Kuntman A, Bahar I, Baysal BM. Macromolecules 1990;23:4959.
[16] Abe A. J Am Chem Soc 1968;90:2205.
[17] Abe A. J Polym Sci Symp 1976;54:135.
[18] Abe A. Macromolecules 1977;10:34.
[19] Mattice WL, Suter UW. Conformational theory of large molecules. New York: Wiley; 1994.
[20] Bacskai R, Pohl HA. J Polym Sci 1960;42:151.
[21] Salovey R. J Polym Sci 1961;50:S7.
[22] Marchal J, Lapp C. J Polym Sci 1958;27:571.
[23] Ando H, Yoshizaki T, Aoki A, Yamakawa H. Macromolecules 1997;30:6199.
[24] Shima M, Sato M, Atsumi M, Hatada K. Polym J 1994;26:579.
[25] Saiz E, Hummel JP, Flory PJ, Plavsic M. J Phys Chem 1981;85:3211.
[26] Tamai Y, Konishi T, Einaga Y, Fujii M, Yamakawa H. Macromolecules 1990;23:4067.
[27] Abe A. J Am Chem Soc 1984;106:14.
[28] Abe A, Jernigan RL, Flory PJ. J Am Chem Soc 1966;88:631.
[29] Bondi A. J Phys Chem 1964;68:441.